

Cambridge University Press

978-1-107-40886-9 - Materials Research Society Symposium Proceedings: Volume 892:  
GaN, AlN, InN and Related Materials

Editors: Martin Kuball, Thomas H. Myers, Joan M. Redwing and Takashi Mukai

Excerpt

[More information](#)

---

## UV and White Light LEDs

Cambridge University Press

978-1-107-40886-9 - Materials Research Society Symposium Proceedings: Volume 892:  
GaN, AlN, InN and Related Materials

Editors: Martin Kuball, Thomas H. Myers, Joan M. Redwing and Takashi Mukai

Excerpt

[More information](#)

---

Cambridge University Press

978-1-107-40886-9 - Materials Research Society Symposium Proceedings: Volume 892:  
GaN, AlN, InN and Related Materials

Editors: Martin Kuball, Thomas H. Myers, Joan M. Redwing and Takashi Mukai

Excerpt

[More information](#)

Mater. Res. Soc. Symp. Proc. Vol. 892 © 2006 Materials Research Society

0892-FF01-01

## Deep Ultraviolet Light Emitting Diodes with Emission below 300 nm

M. Asif Khan

Department of Electrical Engineering, University of South Carolina, Columbia SC 29208, USA

### ABSTRACT

In this paper we will describe the problems in growth and fabrication of deep UV LED devices and the approaches that we have used to grow AlGaIn-based multiple quantum well deep UV LED structures and to overcome issues of doping efficiency, cracking, and slow growth rates both for the n- and the p-type layers of the device structures. Several innovations in structure growth, device structure design and fabrication and packaging have led to the fabrication of devices with emission from 250-300 nm and cw-milliwatt powers at pump currents of only 20 mA ( $V_f \leq 6$  V). Record wall plug efficiencies above 1.5 % are now achievable for devices with emission at 280 nm. Thermal management and a proper device design are not only key factors in achieving these record performance numbers but are also crucial to device reliability. We will also discuss some of our initial research to clarify the factors influencing the lifetime of the deep UV LEDs. In addition to our own work, we will review the results from the excellent research carried out at several other laboratories worldwide.

### INTRODUCTION

At present, several research groups are developing deep ultraviolet light emission devices. The motivation behind this research is the enormous application potential of these devices to be used in bio-medicine, environmental protection, and public health. In addition to being environmentally friendly, LED-based solid state deep UV sources provide significant advantages in size, operation voltage, emission wavelength tunability and control over their conventional counterparts – namely, the mercury vapor lamps.

Fabrication of III-N deep UV LEDs using conventional approaches leads to several major problems. Transparency at the operation wavelengths severely limits the choices of substrates to either sapphire or AlN. In either case one has to resort to heteroepitaxy to deposit the device structures. Deep UV LEDs require active and buffer epilayers of  $\text{Al}_x\text{Ga}_{1-x}\text{N}$  with alloy compositions well over 30%. High Al mole fraction in these layers results in low doping efficiency, cracking, and slow growth rates both for the n- and the p-type layers of the device structures.

In this paper we will discuss approaches such as the use of migration enhanced epitaxy and short period superlattices to overcome the above problems and to fabricate deep UV LED devices emitting at 280 nm with record wall plug efficiency. We will also present results of our studies of device reliability performance and discuss factors affecting the LED reliability. It is shown that such important parameters as junction temperature and pump current density strongly affect long-term LED performance, which can be greatly improved by proper device design and packaging approaches. We will also discuss the development of interconnected micropixel array devices and microlenses for potential microsensing and microdisplay technologies. Along with

our research results we will briefly review research progress made by several other laboratories. Several application areas for deep UV LEDs and some system prototypes will also be discussed.

DEEP UV LED DEVICE STRUCTURE

Generic deep UV LED layer structure is shown in Figure 1. This structure has been suggested by [1,2] and then adopted by many research groups [3-8]. The device epilayer structure was deposited over basal plane sapphire substrates using a combination of metal-organic chemical vapour deposition (MOCVD) and migration enhanced MOCVD (MEMOCVD) techniques. First we used a MEMOCVD process for deposition of the high quality AlN buffer layer.[9] This procedure significantly reduces the screw dislocation density and improves the overall structural quality of the layer. This was followed by an AlN/Al<sub>x</sub>Ga<sub>1-x</sub>N nested superlattice (SL) structure to manage strain in the subsequent AlGaN layers which were grown by conventional MOCVD technique.[10,11] This allows the growth of crack-free n<sup>+</sup>-Al<sub>x</sub>Ga<sub>1-x</sub>N (x>0.3) cladding layers with thicknesses well in excess of 3μm. The multiple quantum well (MQW) active region was deposited on top of the AlGaN cladding layer. It typically consisted of three to five 30-40Å thick AlGaN quantum wells separated with 50-60Å thick AlGaN barriers. The MQW active region was capped with 200Å thick Mg doped AlGaN electron block layer to improve the carrier confinement in the active layer. This was followed with approximately 500Å thick p-AlGaN cladding and p<sup>+</sup>-GaN contact layers. It was shown before that this design of p-AlGaN/p<sup>+</sup>-GaN heterojunction helps increasing the hole injection due to piezo-electric doping.[12] The Al mole fraction in quantum wells was adjusted from ~ 20 to ~ 58% to tune the LED emission wavelength from 340 to 250nm (see for example [13-16]). Simultaneously the Al compositions of AlGaN barrier layers and n<sup>+</sup>- and p-AlGaN cladding layers were also adjusted to preserve the carrier confinement in quantum wells, proper injection conditions and the optical transparency of the cladding layers. The growth pressure was 50 Torr and temperature was 1000-1100 °C. Trimethyl aluminium (TMA), trimethyl gallium (TMG), and NH<sub>3</sub> were used as precursors. SiH<sub>4</sub> and Cp<sub>2</sub>-Mg were used as the n- and the p-type dopants. The p-dopants were activated using a 30 min 800°C annealing.

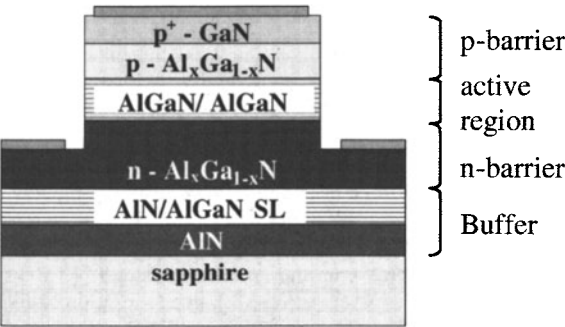


Figure 1. Schematic of deep UV LED on sapphire substrate.

Cambridge University Press

978-1-107-40886-9 - Materials Research Society Symposium Proceedings: Volume 892:

GaN, AlN, InN and Related Materials

Editors: Martin Kuball, Thomas H. Myers, Joan M. Redwing and Takashi Mukai

Excerpt

[More information](#)

It was shown recently that the insertion of SLs between high-quality AlN and n-AlGaN avoids cracking by modifying the strain properties of the epilayer structure and thus significantly improves the electrical properties of n-AlGaN.[17] As shown by cross-section transmission electron microscopy (TEM) and high resolution x-ray diffraction (HRXRD), the AlGaN well material itself in the AlN/AlGaN SL was composed of an  $\text{Al}_x\text{Ga}_{1-x}\text{N}/\text{Al}_{1-y}\text{Ga}_y\text{N}$  short-period superlattice (SPSL), with the periodicity of 15.5 Å ( $\approx$  six monolayer). This phenomenon, which arises from MEMOCVD approach, is believed to be crucial for maintaining coherent growth of the large-period AlN/AlGaN SL for strain/defect management. TEM results, which were recently observed from  $\text{n}^+\text{-AlGaN}$  with a 40-period SL, showed that the screw type dislocation density in  $\text{n}^+\text{-Al}_{0.55}\text{Ga}_{0.45}\text{N}$  is reduced down to  $\sim 7 \times 10^7 \text{ cm}^{-2}$ , whereas the edge type dislocation density was  $\sim 3 \times 10^9 \text{ cm}^{-2}$ . These facts indicate that SL may play a crucial role in a pronounced reduction of screw-type dislocations and/or other defects (such as point defects) and thus significantly improve overall quality of n-cladding AlGaN layers. These results agree well with the measurements of the Hall mobility of n- $\text{Al}_{0.55}\text{Ga}_{0.45}\text{N}$ , which showed the increase of the carrier mobility from 50-70  $\text{cm}^2/\text{V s}$  in n-AlGaN with 5-period SL insertion to 120-130  $\text{cm}^2/\text{V s}$  in n-AlGaN layers with 40-period SL.

After growth wafers were processed with the standard steps, including photolithography, dry etching, and metal evaporation. Mesa structures were formed using chlorine-plasma reactive ion etching. E-beam deposited Ti/Al/Ti/Au n-type ohmic contact metals were annealed in flowing forming gas at 850-950 °C, depending on the n-AlGaN Al-composition. Pd/Ni/Au metals were typically used for p-contact metallization (annealed at approximately 500 °C). Different device geometries have been explored by several groups. These include square [18,19] and round [4] geometry devices, interdigitated finger design [3,20,21], interconnected micro-pixel arrays [13,22] and devices with photonic crystal structures [23]. After processing devices were flip-chip packaged onto ceramic submounts to improve heat dissipation and light extraction. [24,25]

## DEEP UV LED PERFORMANCE

The initial submilliwatt operation of a nitride-based LED emitting at 285 nm was demonstrated in 2002 with a device exhibiting cw output power of 10  $\mu\text{W}$  at 60 mA drive current.[1] Moreover, the emission spectrum consisted of several peaks: a near band-edge emission from the quantum well and long-wavelength peaks associated with deep-level transitions in barrier layers. More recently many groups have reported a significant increase in device output power and spectral purity. Fisher et al. reported dc power levels as high as 1.34 mW at 300 mA for large-area 290 nm devices, while achieving an external quantum efficiency as high as 0.18 % for devices with smaller areas.[3] Recently, Sun et al. and Zhang et al. have demonstrated high-power UV-C LEDs with emission at around 280 nm with a dc output power of approximately 1 mW at 20 mA and a corresponding external quantum efficiency of  $\sim 1.1$  %.[18,19]

LEDs with an emission wavelength at 265–270 nm have also been reported by several groups. Yasan et al. reported submilliwatt dc and pulsed output powers as high as 4.5 mW at 267 nm corresponding to a quantum efficiency of  $\sim 0.1$  %.[26] These powers have been further increased by Adivarahan et al.[27] and Bilenko et al.[28], who have recently reported quantum efficiencies of 0.4 % and 0.2 % at 269 nm and 265 nm, respectively. Submilliwatt pulsed operation of deep UV LEDs with emission wavelength as short as 250 nm was reported by

Cambridge University Press

978-1-107-40886-9 - Materials Research Society Symposium Proceedings: Volume 892: GaN, AlN, InN and Related Materials

Editors: Martin Kuball, Thomas H. Myers, Joan M. Redwing and Takashi Mukai

Excerpt

[More information](#)

Adivarahan et al.[14] Submilliwatt LED operation at 250 nm was also reported for devices structures grown by gas source molecular beam epitaxy.[29] Recently, Allerman et al. have obtained an electroluminescence peak from deep UV LED structure at a wavelength as short as 237 nm, demonstrating the possibility for further reduction of the emission wavelength towards 200 nm.[21]

The dc operation of LEDs with a wavelength shorter than 260 nm becomes severely limited by the lack of conductivity of the bottom Si:doped AlGaN cladding layer since the Al molar fraction required for transparency increases above 70%. To improve current spreading in LEDs with high Al molar fractions in AlGaN cladding layers, an interconnected micropixel design has been adopted. An LED design with interconnected micropixels separated by the n-AlGaN contact metal was also shown to be very efficient in achieving the desired uniform current pumping for deep UV LEDs, and devices with emission at 255 nm with 1 mW dc and 3.4 mW pulse powers and corresponding maximum quantum efficiencies of 0.14 and 0.3 % (in dc and pulse pumping, respectively) have recently been demonstrated.[30]

Great efforts have been made by many groups around the world in developing novel advanced structures for III-nitride deep-UV LEDs resulting now in the successful demonstration of compact and robust solid-state light sources, much needed for a variety of applications. However, the efficiency of deep-UV LEDs is still not comparable to that of near-UV devices. An increase in external quantum efficiency of up to ~ 10 % must be achieved via further improvements of material quality and device optimization. The reduction of defect density and improvements in doping of the AlGaN layers with high Al molar fraction are of great importance for increasing the efficiency of deep-UV emitters and reaching the operation lifetimes of the order of 10,000 h or above at power levels ~ 1 mW. Native single-crystal AlN substrates as well as innovative doping solutions must be considered. Another challenge is light extraction, where novel encapsulation materials that are transparent down to ~ 200 nm should be explored.

## CURRENT RESEARCH TRENDS

With ongoing development and initial commercialization of deep UV LED long term device reliability becomes a very important issue. Sufficiently high density of threading dislocations in AlGaN layers, lower conductivity and inherently high operating voltage and high current density potentially lead to limited device operation lifetime. Only limited studies have been done to analyze the reliability of deep UV LEDs. Thus we discuss some of recent our work on reliability performance.

For analysis of LED reliability we used unpackaged devices to eliminate the contribution of bonding interfaces and solder and to focus on LED degradation process only. Output power and emission spectrum were first measured from the sapphire substrate side placing the sample on either calibrated photodetector or optical fiber bundle connected to a spectrometer. During the stressing the sample was mounted on temperature controlled chuck and relative power level was monitored from the top side of wafer. For this study the unpackaged AlGaN-based LEDs had a starting optical output power of 0.35 mW, external quantum efficiency of about 0.4%, and the peak emission at 280 nm at 20 mA. The long wavelength emission was more than 3 orders of magnitude lower than the 280 nm main emission.

For the reliability measurements the relative optical power was monitored as a function of time under constant current conditions. Devices were typically stressed at 20 mA, which

translated to a relatively high current density of 200 A/cm<sup>2</sup> for 100 μm x 100 μm square devices. The thermal impedance for unpackaged device was measured to be around 180 °C/W, which is considerably higher than that measured for flip-chip bonded devices (33 °C/W) as confirmed by the LED operating voltage shift [31] and electroluminescence spectrum peak shift.[32] Thus, we estimate the junction temperature rise around 24.5 °C above the ambient temperature at the bias current of 20 mA and operating voltage of 6.8 V.

The aging tests were also performed under dc current stress at different chuck temperatures. Each aging test was performed for 24 hours under constant current of 20 mA. Figure 2 shows the decay of the LED optical power as a function of time and temperature. From the stress data obtained under pulsed pumping conditions with low (≤5%) duty cycle for various pump current and temperature conditions it was found that optical power decay is caused by both an increase in the junction temperature and the high pump current density (not shown). Thus, each curve of Figure 2 was fitted using a double-exponential decay function as:

$$P(t) = P_1 \exp(-\beta_1 t) + P_2 \exp(-\beta_2 t), \tag{1}$$

where  $P_1$  and  $\beta_1$  were assigned as temperature dependent parameters,  $P_2$  and  $\beta_2$  were bias dependent parameters. Temperature dependent decay part changes exponentially with junction temperature  $T_J$  as:

$$\beta_1 = \beta_0 \exp(-E_a / kT_J), \tag{2}$$

with the activation energy  $E_a$  of 0.27 eV and decay parameter  $\beta_0$  of 97.5 h<sup>-1</sup> as found from the Arrhenius plot. Thus the value of decay parameter  $\beta$  of  $5.93 \times 10^{-3}$  h<sup>-1</sup> can be estimated for an unpackaged device biased at 20 mA dc at room temperature. The value of parameter  $\beta_2$ , which did not show clear temperature dependence, was determined to be about 0.44 h<sup>-1</sup>.

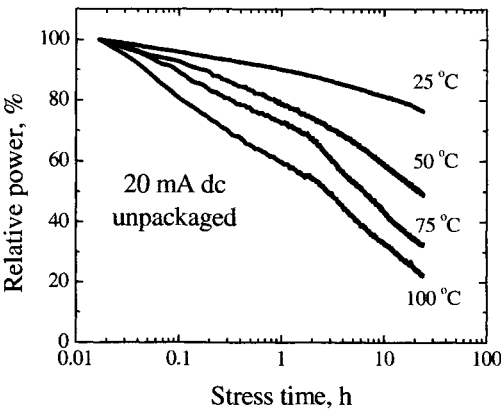


Figure 2. Optical power decay during long term stress at various temperatures for 280nm unpackaged deep UV LED.

We also performed aging studies on 10x10 micro-pixel 280nm emission deep UV LEDs. Details of interconnected micro-pixel array LED can be found elsewhere.[13] Based on reliability studies described above the performance of micro-pixel devices is expected to improve due to the following factors: i) lower current density (at 20mA) due to larger device area; ii) lower operating voltage due to a lower series resistance; iii) lower junction temperature due to (ii) and a lower thermal impedance. For this study devices were flip-chip mounted onto TO-66 headers for thermal management. At 20 mA dc pump current the 10x10 micro-pixel design LED showed the operating voltage to be 0.7V lower than that for 200  $\mu\text{m}$  x 200  $\mu\text{m}$  square device and 1.2V lower than that for standard 100  $\mu\text{m}$  x 100  $\mu\text{m}$  square device. For devices with larger area the contribution of p-contact specific contact resistance to the LED differential resistance is smaller, which leads to the reduction of the operating voltage. For the devices with equal area (200  $\mu\text{m}$  x 200  $\mu\text{m}$  square and 10x10 micro-pixel) further reduction of the differential resistance is achieved due to reduction of current crowding in micro-pixel LED design. As follows from the stress data presented in Figure 3, the four-fold increase of the junction area led to improved reliability performance of micro-pixel LED with the projected operation life-time for 50% power reduction in excess of 1000 hours.

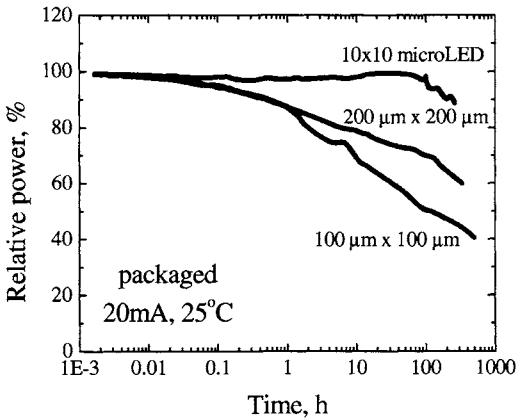


Figure 3. Packaged LED long term stress at 20 mA dc and 25 °C ambient temperature.

Another area of emerging research is the use of micro- and nanostructures for enhanced light extraction and light focusing. Khizar et al. reported the enhancement of UV LED efficiency by using micro-patterned sapphire substrates.[33] Diamond and polymer microlenses were also reported for visible and near-UV LEDs to collimate the light output especially in micro-pixel design devices, which ultimately can be used for creation of micro-sensors and micro-displays.[34,22]

We now report the development of UV transparent planar Fresnel microlenses over sapphire substrates. Lenses were formed on sapphire surface using a  $\text{SiO}_2$ -based coating material patterned by direct e-beam writing. SEM image of Fresnel microlens is shown in Figure 4.



Cambridge University Press

978-1-107-40886-9 - Materials Research Society Symposium Proceedings: Volume 892:

GaN, AlN, InN and Related Materials

Editors: Martin Kuball, Thomas H. Myers, Joan M. Redwing and Takashi Mukai

Excerpt

[More information](#)

Lenses with diameter of  $33\text{ }\mu\text{m}$  consisted of 8 rings. Vertical step-like profile of each ring was achieved through multiple exposures so that each ring had maximum thickness of  $560\text{ nm}$  graded in 4 steps to zero thickness. This geometry was calculated to provide the focal distance of  $60\text{ }\mu\text{m}$  at  $280\text{ nm}$  wavelength. Optical properties of these Fresnel lenses were initially studied using confocal microscope (not shown). Since the microscope was only capable to operate in the range from  $400\text{ nm}$  to  $600\text{ nm}$ , thus we have used commercial green ( $530\text{ nm}$ ) LED as a light source. Lens design was optimized for  $280\text{ nm}$  wavelength with  $4\pi$  maximum phase shift, therefore it worked well for a green LED providing  $2\pi$  maximum phase shift.

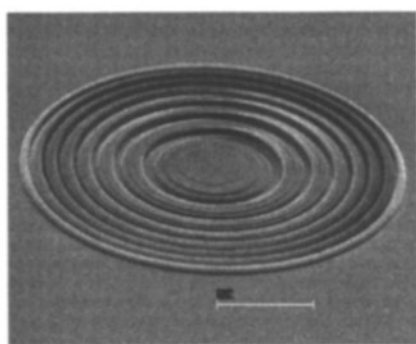


Figure 4.  $\text{SiO}_2$  based Fresnel microlens on sapphire substrate. Scale bar is  $10\text{ }\mu\text{m}$ .

Finally, the array of microlenses was fabricated on the back side of the fully processed wafer consisting of micro-pixel geometry LEDs. Lens geometry was chosen such that each lens was aligned across each micro-LED pixel. The focusing performance of the lens was verified by UV-transparent microscope and UV-enhanced CCD camera. In Figure 5 we include the CCD images taken from the back side of the sapphire substrate. UV emission from the micro-pixel was passing through the sapphire substrate falling onto the micro-lens and focusing into a spot. As seen from Figure 5 (a), when microscope objective lens is focused onto the emission plane the emission pattern forms a round spot corresponding to the size of the micro-pixel. When microscope is focused on the lens plane (back side surface of the sapphire) the fine structure of the Fresnel lens can be resolved (Figure 5 (b)). The area around the lens is illuminated due to light divergence in the substrate. When the microscope is further detuned from the emission plane (into the air), the emission focuses into a tight spot corresponding to the focal plane position (Figure 5 (c)). The focal distance of the actual lens was found to be  $68.5\text{ }\mu\text{m}$ , which is very close to the calculated value of  $60\text{ }\mu\text{m}$ .

Cambridge University Press

978-1-107-40886-9 - Materials Research Society Symposium Proceedings: Volume 892:  
GaN, AlN, InN and Related Materials

Editors: Martin Kuball, Thomas H. Myers, Joan M. Redwing and Takashi Mukai

Excerpt

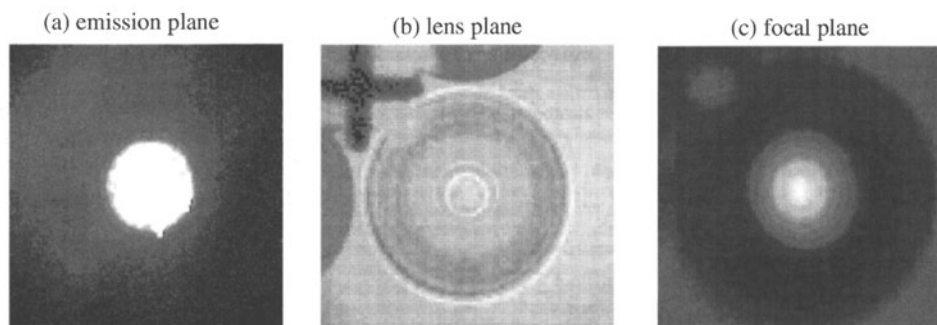
[More information](#)

Figure 5. UV CCD images of the emission from single micro-pixel taken through the Fresnel microlens from the back side of the sapphire substrate.

## APPLICATIONS

Impressive research efforts in development of III-nitride UV devices have resulted in operation over a wide range of UV wavelengths spanning from near UV to deep UV. These UV LEDs have started to find their applications in fluorescence-based biochemical sensing, covert communications, purification and disinfection. Several UV LED based system prototypes have been reported. A prototype bioagent detection system based on time resolved fluorescence of fluorophores such as tryptophan and NADH excited with 280 nm and 340 nm UV LEDs, respectively was reported by Peng et al. [35], Han et al. [36], and Li et al. [37]. Frequency domain and time domain measurements of fluorescence lifetimes of several natural organic fluorophores have also been published recently. [38,39] Successful demonstration of non-line-of-sight (NLOS) optical covert communication link operating at bit rates of several kbps was established between deep UV LED based optical source and photomultiplier-based receiver both operating in solar-blind ( $\lambda < 280$  nm) region. [40] Zenith-pointed transmitter and receiver were used to exploit isotropic atmosphere molecular scattering for NLOS transmission in solar-blind region, where the background solar radiation does not contribute to the receiver noise. Finally, germicidal action of UV emission was also explored by several groups who reported prototypes of flowing water purification reactors with bacteria killing efficiencies of up to 99.996 %. [41,42]

## CONCLUSIONS

Rapid development of deep UV LEDs led to fabrication of devices with emission wavelength below 300nm, exhibiting wall-plug efficiency of up to ~1.5%. These devices are already proven to be suitable for bio-sensing, communication and water purification applications. The development of alternative precursors for MOCVD growth of AlGaN may improve control of heteroepitaxy and minimize impurity incorporation. The development of native substrates for homoepitaxy of GaN and, especially, AlN layers are expected to lead to next-generation devices with higher efficiencies.